19th Brazilian Congress of Thermal Sciences and Engineering
November 06th-10th, 2022, Bento Gonçalves - RS - Brazil

ENC-2022-0200
RADIATOR IMPACT ON STIRLING CYCLE EFFICIENCY FOR SPACE POWER GENERATION

Ermerson Ferreira de Moura[1]
Guilherme Borges Ribeiro[2]
Izabela Batista Henriques[3]
Aeronautics Institute of Technology, São josé dos Campos, Brazil.
ermerson@ita.br[1], gbribeiro@ita.br[2], izabela@ita.br[3]

Abstract. *With the increasing ambition of space agencies and the private sector, space missions are increasingly daring and focus on deep space missions, aiming to reach planets like Mars and Jupiter. For missions with these objectives to be viable, the spacecraft must have a high availability of energy to carry out the mission safely. Although solar conversion systems are well established for space application, they have a number of limitations such as the low solar incidence on more distant planets would make it impossible to apply a photovoltaic system. In this scenario, nuclear power generation systems are an alternative, as they can operate for long periods providing a high amount of energy. However, for these systems to become applicable, an energy conversion system with high efficiency and low mass must be applied. Dynamic conversion cycles, especially the Stirling cycle, is one of the best options, however, several components considerably increase the system mass, especially the radiator. This component used for heat rejection, can be responsible for more than 1/3 of the entire system mass. Considering this perspective, this work performed a finite time thermodynamic modeling of a Stirling cycle and an exergy analysis to evaluate the radiator impact on the system. With the model, it was possible to evaluate the impact of the radiator area on the cycle energy and exergy efficiency, map the radiator irreversibility; find the ratio of the increase in radiator mass to the increase in panel area; and through a figure of merit to find the best kg/kW system ratio that provides the greatest efficiency. With the results it was possible to identify that with approximately 70 m² of radiator area the system finds the best kg/kW ratio. These results may provide valuable theoretical insight into the future development of radiators for space nuclear power conversion systems.*

Keywords: *Radiator, finite-time thermodynamics, efficiency, stirling, power generation.*

1. INTRODUCTION

In the coming years there is a prospect of constant growth in the aerospace sector. New missions like the man-to-moon return in NASA's Artemis program and intentions by private companies to reach outer planets like Mars ignite demand for systems that can support missions of this complexity. For missions like this to be possible, the first challenge is high-reliability and energy-density power generation systems for space (Moura et al. 2022, Fan et al. 2017, Fan et al. 2018). The systems used or that are seen as an alternative are photovoltaic, nuclear, and chemical systems.. (Moura et al. 2021a, Araújo et al. 2018). The generation of photovoltaic energy is shown as an alternative for the supply of power for long periods, but its application is limited to solar incidence, and for missions further away from the sun or in inhospitable environments, its use becomes unfeasible. (Araujo et al. 2018, Dai et al. 2020, Fan et al. 2017). Chemical energy delivers a large amount of energy in a short period, and its application is aimed at accessing space and not deep space missions because they are longer missions (for a mission on Mars, a period between 2 to 3 years is estimated).Within this perspective, nuclear power generation is one of the most promising in view of the high energy density delivered by these systems compared, and the great availability over time (its operability can be extended for more than 10 years according to Mcclure et al. (2013)) without depending on environmental conditions, allows its application to inhospitable environments far from Earth, such as missions to Saturn and Jupiter. (Moura et al. 2021b, Fan et al. 2018, Dai et al. 2019, Dai et al. 2020).

Nuclear power generation systems can be classified between static systems and dynamic systems. Static systems do not use moving parts, but their efficiency is low, not exceedingly approximately 10% (Fan et al. 2017, El-Genk et al. 2008a, El-Genk et al. 2008b, El-Genk et al. 2008b, El-Genk et al. Genk et al. 2011). Dynamic systems have an efficiency of around 20 to 30% and are seen as the best option for high power demanding space applications (Moura et al. 2020, Ribeiro et al. 2015, Gallo et al. 2009, Juhasz et al. 2007). Dynamic nuclear power generation systems have as main

components the presence of a nuclear reactor, hot heat pipes (HHP), power conversion system (Brayton, Stirling, or Rankine), and the heat rejection system (heat pipe-radiator assembly).

Among the dynamic nuclear energy conversion cycles for space applications the Stirling cycle is the one of the best options, comparing with the Brayton cycle, while the Brayton cycle reaches 40% with a temperature ratio between 3 and 4, the stirling engine can reach 60% of the efficiency of an ideal Carnot with a temperature ratio between 2 and 3 (Lee et al. 2007). The typical Stirling engine for space applications contains a heater (hot side), cooler (cold side), piston, displacer, expansion space, compression space, regenerator, casing, support structure and linear alternators (Dai et al. 2020).

The use of dynamic systems increases the number of system's failure modes, by increasing the number of moving parts. For space applications, reliability is essential, since if the system ceases to be operational, the mission will fail and, if manned, it can put human life at risk, within this perspective, the Free Piston Stirling Engine (FPSE) in beta configuration is used for space applications (Maxwell, 2016). An FPSE is dynamically coupled to the gas, but not mechanically, with no crank mechanism in the arrangement. In the beta configuration, the engine structure is designed so that the piston and displacer are positioned on the same cylinder (Ahmadi et al. 2017). In this way, the number of moving parts is reduced, increasing the engine reliability. The working fluid commonly used is helium due to the low density, high thermal conductivity, low viscosity and high specific heat, enhancing the cycle performance (Fan et al. 2017, Dai et al. 2020).

The heat exchange present in nuclear power generation systems in space and through radiation. The assembly of heat pipes-radiator can correspond to more than 1/3 of the system mass and its optimization is strictly necessary for the system to have a better mass-to-power ratio. Within this perspective, this work aims to analyze the impact of the radiator area on the system energy density and, through a figure of merit Ω, find the best kg/kW ratio for the system in this configuration. Still, a Stirling engine exergy analysis as a function of the radiator area will be carried out, to map radiator irreversibility and its global impact on the system.

2. THERMODYNAMIC MODEL

The thermodynamic model adopted for this work is based on the finite-time thermodynamics approach. Thus, this model deals with processes that have explicit time or rate dependencies (Andresen et al. 1996). For the thermodynamic modeling, the following assumptions are made:

- the specific heat of the working fluid is constant.
- the working fluid is modeled as an ideal gas.
- the regenerative process is imperfect, with uniform temperature distribution.
- the model is steady state with prescribed time.
- the heat transfer between the reactor core and the hot heat pipes occurs by conduction.
- heat conduction leads to a heat loss between the hot side and cold side of the Stirling cycle.

In Figure (1), a T-s diagram is displayed, detailing the heat transfer and the thermodynamic processes involved in a typical Nuclear Stirling conversion system for space applications.

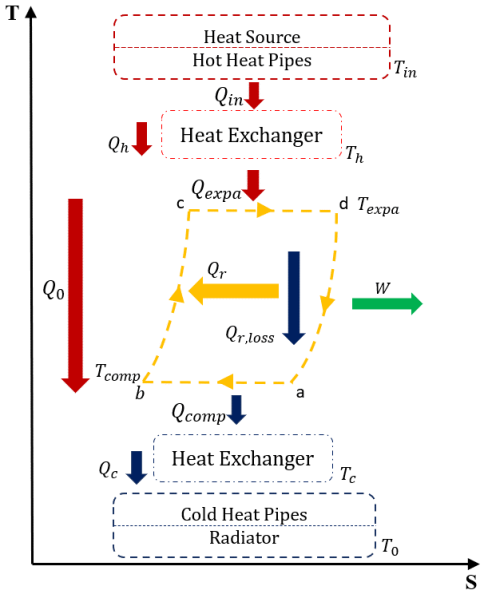

Figure 1. T-S diagram of nuclear Stirling engine with the heat flows and losses.

In this model, the temperature T_H is the difference between the temperature of the core and the temperature drop ΔT_{hp} of the hot heat pipe according to equation (1). The temperature drop calculation is obtained through a one-dimensional heat pipe model presented by Romano et al (2019, 2020, 2021) and also presented by Moura et al.(2020). In this model, the thermal conductance in each region of the heat pipe is computed, as well as the temperature drop. For the heat model, the following HP limits are respected: the capillary, boiling, entrainment, sonic and viscous limit (Zohuri et al. 2016). For the sake of conciseness, further details about the HP modeling can be seen in the aforementioned studies. Thus, we have

$$T_H = T_I - \Delta T_{hp} \tag{1}$$

The thermal bridge between the hot and cold side of the Stirling engine is proportional to the temperature difference and the cycle time (τ), being described by the following equation (Fan et al. 2017).

$$Q_0 = \nu_o (T_H - T_C)\tau \tag{2}$$

where ν_o is the heat leak coefficient between the hot and cold side, and T_C is the cold side temperature. In this model, finite heat transfer through the regenerator is considered. The regenerative processes are affected by the internal thermal resistances in the regenerator. Thus, there are regenerative losses per cycle during the two regenerative processes. The regenerative heat transfer is proportional to the temperature difference of the working fluid, and can be described as (Shubhash et al. 2014):

$$Q_r = nc_v\varepsilon_r\left(T_{expa} - T_{comp}\right) \tag{3}$$

where n is the number of moles of Helium, c_v is the specific heat on a molar basis, ε_R is the efficiency of the regenerator, and T_{expa} and T_{comp} denote the expansion and compression temperatures, respectively. Considering the fractional deviation from the ideal regeneration, the heat loss Q_R in the regenerator can be described as follows (Shubhash et al. 2014):

$$Q_{r,loss} = nc_v(1 - \varepsilon_r)\left(T_{expa} - T_{comp}\right) \tag{4}$$

The convective heat transfer is assumed to be the main heat transfer mechanism between the heat exchangers and the working fluid. Thus, the amount of heat absorbed by the working fluid on the hot side and released to the cold side can be described by the following equations (Shubhash et al. 2014):

$$Q_{expa} = UA_{hc}\left(T_H - T_{expa}\right)\tau_1 = nRT_{expa}ln\lambda + nc_v(1 - \varepsilon_r)\left(T_{expa} - T_{comp}\right) \tag{5}$$

$$Q_{comp} = UA_{cc}\left(T_{comp} - T_C\right)\tau_2 = nRT_{comp}ln\lambda + nc_v(1 - \varepsilon_r)\left(T_{expa} - T_{comp}\right) \tag{6}$$

where Q_{expa} is the amount of heat absorbed by the working fluid, Q_{comp} is the amount of heat released by the working fluid, R is the universal gas constant; UA_{HC} is the thermal conductance of the hot side heat exchanger, UA_{CC} is the thermal conductance of the cold side heat exchanger; and λ is the compression ratio, being described as follows

$$\lambda = \frac{V_{comp}}{V_{expa}} \tag{7}$$

where V_{comp} is the volume of the compression side and V_{expa} is the volume of the expansion side. The periods of the processes of expansion and compression, τ_1 e τ_2, respectively, can be described as

$$\tau_1 = \frac{nRT_{expa} ln\lambda + nc_v(1-\varepsilon_r)(T_{expa} - T_{comp})}{UA_{hc}(T_H - T_{expa})} \tag{8}$$

$$\tau_2 = \frac{nRT_{comp} ln\lambda + nc_v(1-\varepsilon_r)(T_{expa} - T_{comp})}{UA_{cc}(T_{expa} - T_C)} \tag{9}$$

The total cycle period is the sum of the time of the four processes. Thus, we have

$$\tau = \tau_1 + \tau_2 + \tau_3 + \tau_4 \tag{10}$$

where the periods τ_3 and τ_4 denotes the period of each isochoric process that occur in the regenerator. These periods can be calculated with the model presented by Dai et al. (2018) as follows

$$\tau_3 = \frac{\ln\left[1 - \left(1 + \frac{C_r}{C_f}\right)\frac{T_{expa} - T_{comp}}{T_{expa} - T_C}\right]}{-\alpha_r\left(\frac{1}{C_r} + \frac{1}{C_f}\right)} \tag{11}$$

$$\tau_4 = \frac{\ln\left[1 - \left(1 + \frac{C_r}{C_f}\right)\frac{T_{expa} - T_{comp}}{T_H - T_{comp}}\right]}{-\alpha_r\left(\frac{1}{C_r} + \frac{1}{C_f}\right)} \tag{12}$$

where C_r and C_f are the regenerator and fluid heat capacities, respectively, being $C_f = m_f c_v$, m_f is the fluid mass and c_v is the specific heat of the working fluid at constant volume. Moreover, α_r denotes the regenerator heat transfer coefficient. For this model, it will be assumed that the thermal conductivity of the regenerator is sufficiently large, allowing the temperature distribution to be uniform. The heat transfer coefficient of the working fluid and the regenerator varies with time. Thus, the regenerator effectiveness can be defined as

$$\varepsilon_r = \frac{T_{expa} - T_C}{T_H - T_C} = \frac{T_h - T_{comp}}{T_H - T_C} \tag{13}$$

The engine hot side heat is the combination of the heat from the expansion process adding the thermal bridge. And the heat from the engine cold side is the sum of the heat from the compression process plus the thermal bridge. Therefore, the equations can be described, respectively, as follows:

$$Q_H = Q_{expa} + Q_0 \tag{14}$$

$$Q_C = Q_{comp} + Q_0 \tag{15}$$

Considering the cycle period of the Stirling engine τ, the system power output $\dot{W}$ can be computed as

$$\dot{W} = \frac{W}{\tau} = N_{stg}\frac{Q_H - Q_C}{\tau} \tag{16}$$

where N_{stg} the number of Stirling engines. The cycle energy efficiency η_t is obtained as

$$\eta_t = \frac{Q_h - Q_c}{Q_h} \tag{17}$$

In this modeling, there is a coupling between the thermodynamic model mentioned above and a dynamic model that allows calculating the displacements of the piston and the displacer as a function of process time τ. However, to calculate the τ it is necessary to know the compression ratio, however, it is necessary to know the displacement of the piston and the displacer and as mentioned it is a function of the process time. Thus, to obtain a solution, both models must be solved in a coupled manner through a numerical method that allows the computation of both variables. For the sake of conciseness, further details about the dynamic modelling can be seen in the follow studies: Moura et al. (2021a,2021b,2022).

As already discussed, the mechanism of heat exchange in space is thermal radiation. Therefore, to determine the area of the radiator panel, the following equation is used Siegel (1981):

$$Q_{rad} = \xi \sigma A_{pa}(T_{rad}^4 - T_0^4)\tau \tag{18}$$

where T_{rad} is the radiator temperature, computed based on the average temperature of the condensing and evaporating region of the cold heat pipes attached to the radiator. The variables ξ and σ denote the radiator emissivity and the Stefan-Boltzmann constant, respectively. For this modeling, the wasted heat Q_{rad} is exactly equal to the heat on the cold side of the engine Q_c. Additionally, the cold heat pipes have physical contact with the radiator panels, consisting in a heat pipe-radiator assembly. Considering a conical shape similar to the Kilopower project Maxwell et al.(2018), the final radiator area is computed as follows:

$$A_{rad} = N_{hp,c}\left(\pi r_{rad}^2 - \pi r_{hp}^2\right) + \pi L_{pa} r_{pa} \tag{19}$$

where $N_{hp,c}$ is the number of cold heat pipes, r_{rad} is the radius of the structure surrounding the heat pipe, r_{hp} is the external radius of the heat pipe, L_{pa} is the panel length, and r_{pa} is the panel radius. According to Tarlecki et al. (2007), the heat pipe-radiator assembly is responsible for the largest percentage of mass and area in a typical space power system, being responsible for almost a third of the total mass of the energy conversion system Juhasz (2007). In this way, a figure of merit is implemented to identify the optimized cold side temperature of the Stirling cycle. Therefore, the figure of merit Ω (kg. kW^{-1}) is defined as the ratio of the total mass of the system to the power output, based on the following expression:

$$\Omega = \frac{m_s}{\dot{W}\, N_{stg}} \tag{20}$$

where m_s is the mass of the energy conversion system, consisting of the nuclear reactor core, radiator, and the Stirling engines. The mass of the system is calculated as follows:

$$m_s = (m_{core} + m_{stg} + m_{rad})1.15 \tag{21}$$

where the m_{core} is assumed as 5.82 kg. kW^{-1} according to Fan et al. (2017). Furthermore, an increase of 15% of the mass is considered, corresponding to the power processing and cabling Noca (2001). The variable m_{stg} is the total mass of Stirling engines, and m_{rad} is the radiator mass. For determination of radiation exergy, as mentioned by Petela (1964), a process of simultaneous emission and absorption of radiation is always an irreversible process for temperatures above 0 K. For the rate of exergy transfer per area associated with radiation, considering a perfectly gray body, the following equation is used:

$$\Upsilon_{rad} = \xi \frac{\sigma}{12}(3T_{rad}^4 + T_0^4 - 4T_0 T_{rad}^3) \tag{22}$$

being σ is the Stefan-Boltzmann constant, and ξ is the emissivity. To compute the radiator irreversibility, the exergy provided by cold heat pipes that exchange heat with the radiator, added to the radiation exergy, is taken into account. Thus, the irreversibility and the exergy efficiency of the heat pipe-radiator assembly are described as follows:

$$I_{rad} = \left(1 - \frac{T_0}{T_c}\right) Q_c - \xi \frac{\sigma}{12} A_{rad}(3T_{rad}^4 + T_0^4 - 4T_0 T_{rad}^3)\tau \tag{23}$$

For the Exergy of the Stirling engine, the follow equation is used:

$$\eta_{exe} = \frac{W}{\left(1 - \frac{To}{T_H}\right) Q_H} \tag{24}$$

3. RESULTS AND DISCUSSION

To verify the best characteristics for these systems, the following parameters will be kept constant, as seen in table 1:

Table 1. – Inputs used for the stirling cycle.

Variable	Value	References
UA_{CC}(Cold overall Thermal conductance)	$200\ W/K$	Fan et al. (2017)
UA_{HC} (Hot overall thermal conductance)	$200\ W/K$	Fan et al. (2017)
n (mols)	$1\ mol$	Fan et al. (2017)
ε_r (regenerator effectiveness)	0.9	Fan et al. (2017)
R (Universal gas constant)	$8.314\ J/Mol.K$	Fan et al. (2017)
v_0(Heat leak coefficient)	$2.5\ W/K$	Fan et al. (2017)
c_v (Work fluid specific heat)	$12.5\ J/mol.K$	Dai et al. (2018)
T_I (Heat source temperature)	$1200\ K$	Fan et al. (2017)
T_0(Environment temperature)	$150\ K$	Author's decision
T_c (Temperature of cold side)	$300\ K$	Author's decision
α_r (Regenerator heat transfer coefficient)	$500\ W/m.K$	NASA Lewis Center (1999)
N_{stg} (Number of Stirling Engines	8	Author's decision

For the hot heat pipes, it will be considered that the container material is niobium, and the working fluid is lithium. The temperature of the space in regions close to the earth can vary from 393 K to 100K. In this work, a fixed temperature of 150 K was defined as the environment temperature. The number of heat pipes on the hot side is 150, based on the proportion of heat pipes in the reactor core presented by Fan et al. (2017).

In order to understand the impact of the engine's cold side temperature on the radiator area, in the figure (2) the radiator area is calculated for temperatures from 274 K to 600 K. As can be seen, Increasing the temperature reduces the radiator area. This occurs because the radiator area is dependent on the heat T_C which in turn depends on the heat Q_C.

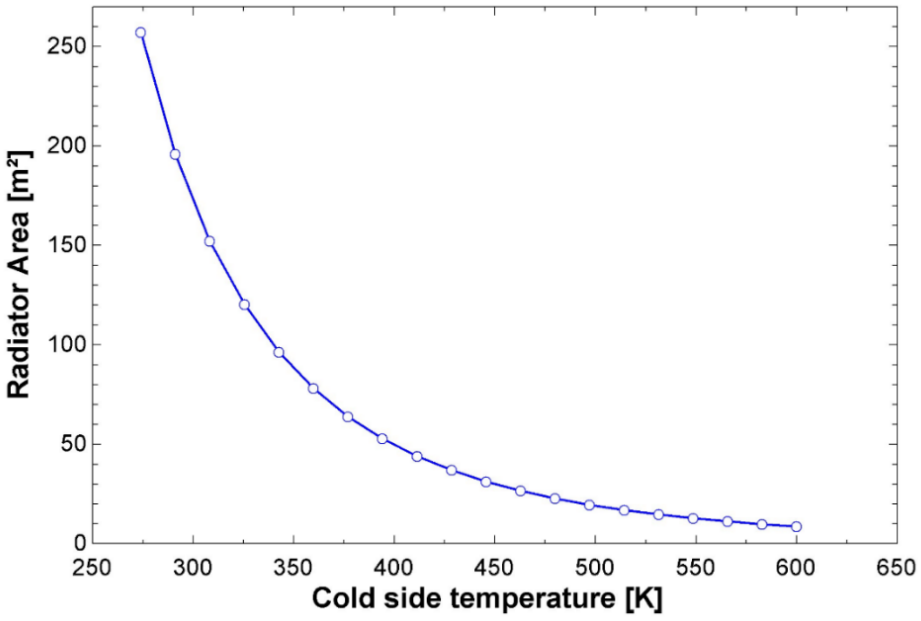

Figure 2. Radiator area as a function of the cold side temperature.

In order to analyze the impact of increasing the radiator area on the energy and exergy system, the figures (3a) and (3b) present the behavior of both efficiencies for different values of A_{rad}. Compared to energy and exergy efficiency for the same temperature, the exergy efficiency is higher than the energy. Analyzing the equation (24) of the cycle exergy efficiency and compared with the cycle energy efficiency equation (17), it is visible that the exergy input is a fraction of the energy input. Therefore, in this case, exergy efficiency is greater than energy, but the work is the same for both cases. In some cases, exergy can be a more important indicator than energy. Systems with high exergy efficiency imply high quality energy used in the system.

Furthermore, it is apparent that increasing the radiator area considerably increases the system efficiencies, as increasing this area will increase the value of Q_c. Also, it is possible to see that there is a more significant impact for increasing the radiator area up to approximately 70 m², for larger increases the efficiency gains are marginal considering the large growth in area.

In order to evaluate the impact of the increase in the area on the radiator irreversibility, figure (3) presents the result for the behavior of the radiator irreversibility the increase of its area. As the radiator area rises, the system irreversibility tends to decrease, as the heat rejection becomes more efficient because with the larger area the temperature differences along the radiator become smaller, and a higher heat rate can be rejected which reduces irreversibility. However, as seen in the previous results for values of areas greater than 70 m², the reduction in irreversibility obtained is small compared to the large increase. This behavior is associated with the thermodynamic limitations of the second law.

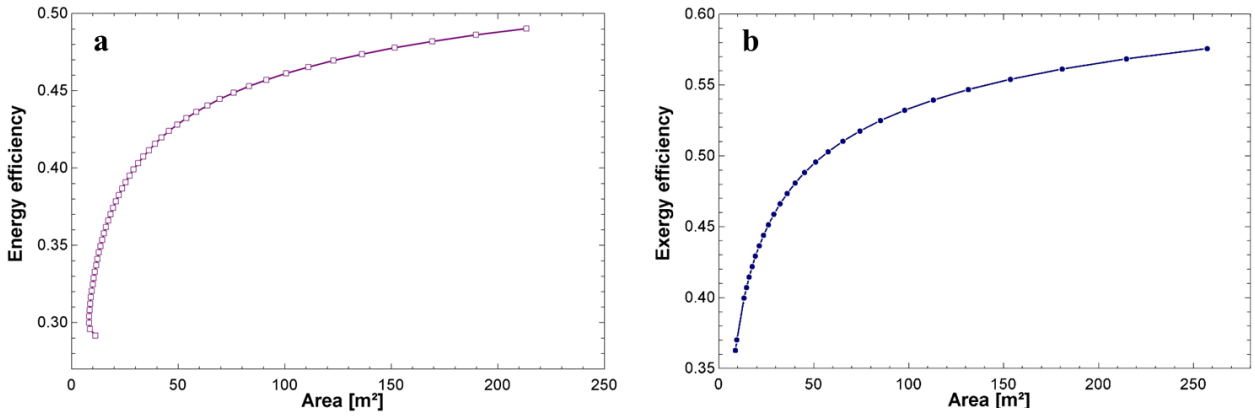

Figure 3. Energy efficiency as a function of the radiator area (a), Exergy efficiency as a function of the radiator area (b).

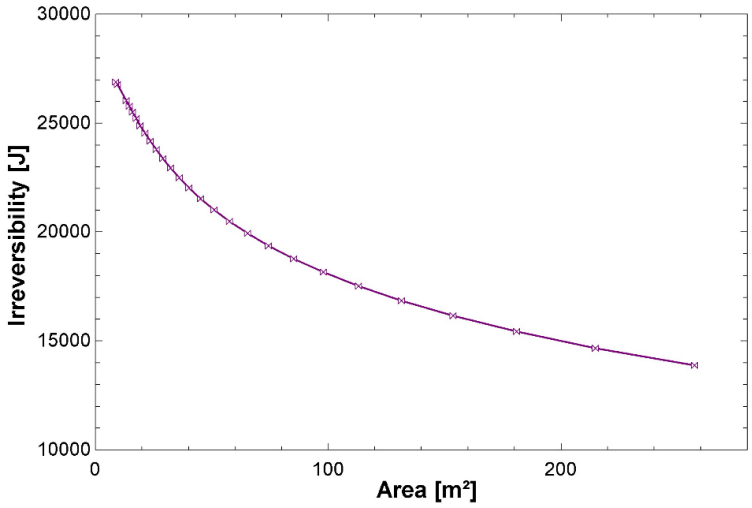

Figure 4. Radiator Irreversibility as a function of the radiator panels area.

In figure (5) the impact of the radiator panel area in the heat-rejection system mass is clear. With an area of 153.6 m², the mass is equal to 1686 kg while with an area of 8.663 m² the rejection system mass is 163.4 kg. Up to a temperature of 375 K (equivalent to 65 m²), the increase in the radiator area is less with a reduction in temperature than seen for temperatures below 350 K, as seen in figure (5).

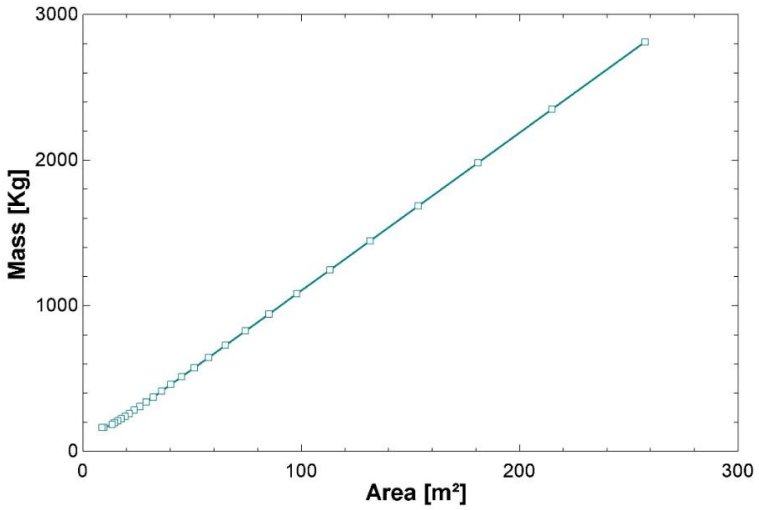

Figure 5. Radiator mass as a function of the Radiator area.

In figure (6) the system is evaluated for an increase in the radiator area. With a very large radiator area the power increases, but as a result the system mass increases in large proportion, on the other hand, for a small radiator area the system power is low. As power and mass are conflicting quantities it is essential to find the optimal point of this ratio, for this system with approximately 70 m² (354.2 K) radiator area, the system has the best mass-to-power ratio obtained by figure of merit Ω. This relationship evaluated by Ω is fundamental for space applications due to the limitations for launching systems in orbit, something that is not analyzed for terrestrial nuclear power generation systems.

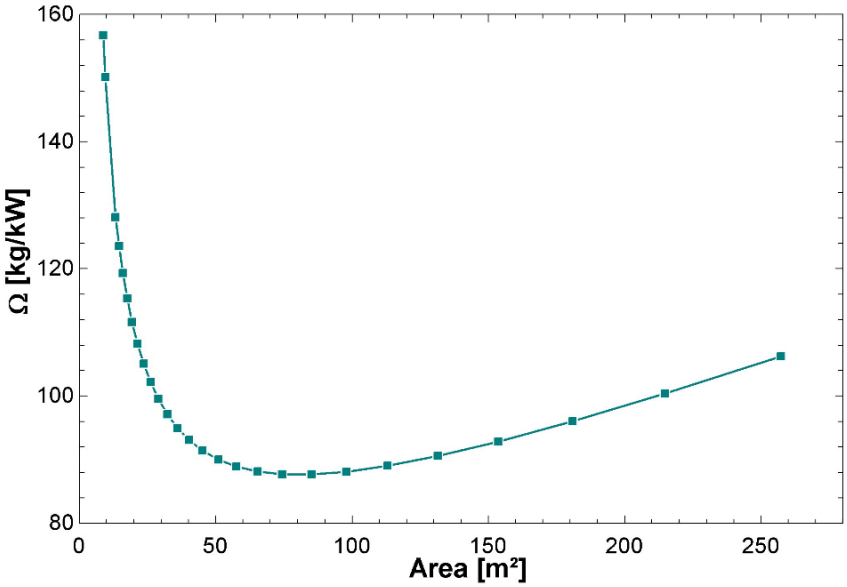

Figure 6. Figure of merit (kg/kW) as a function of the radiator area.

4. CONCLUSION

In the present work, a finite-time thermodynamic modeling was performed to analysis nuclear-powered Stirling engine for space power generation. From the model developed, it was possible to identify the increase in the cold side temperature considerably decreases the radiator area, however, it will consequently reduce the system power by reducing

the heat rejected. On the other hand, rising the radiator area considerably increases the engine efficiency and reduces its irreversibility, however, the system mass increases considerably. In this way, a merit figure (Ω) was applied to find the point of the best system mass per power ratio as a function of the radiator area. Therefore, it was possible to identify that with a radiator area of approximately 70 m², the system has the best kg/kW, which is fundamental for space applications.

Therefore, taking into account the results obtained, this study can provide significant baselines for the future development and analysis of heat rejection systems for space applications.

5. REFERENCES

1. Ahmadi, M. H., Ahmadi, M.-A., Pourfayaz, F. "Thermal models for analysis of performance of Stirling engine: A review". Renewable and Sustainable Energy Reviews, 68, (2017) 168–184. doi:10.1016/j.rser.2016.09.033.
2. Ahmadi M.H, Sayyaadi H., Dehghani S., Hosseinzade H. "Designing a solar powered Stirling heat engine based on multiple criteria: maximized thermal efficiency and power". Energy Convers. Manage 75 (2013) 282–291.
3. Andresen, B. "Finite-time thermodynamics and thermodynamic length". Revue Générale de Thermique. 35(418-419), 1996, 647–650.
4. Araújo E.F, Guimarães L.N.F. "American Space Nuclear Electric Systems". J Aerosp Technol Manag. (2018) 10:e4418.
5. Berchowitz D. M. "A Phasor Description of the Stirling Cycle". The International Stirling Engine Conference (ISEC 2016) Available in: < https://www.ohio.edu/mechanical/stirling/ISEC_papers/ISEC2016-Berchowitz.pdf> Access in: 05/11/2020
6. Dai D.D, Yuan F., Long R., Liu Z.C., Liu W. "Imperfect regeneration analysis of Stirling engine caused by temperature differences in regenerator". Energy Conversion and Management 158 (2018) 60–69.
7. Dai, Z., Wang, C., Zhang, D., Tian, W., Qiu, S., Su, G.H. "Thermoelectric characteristics analysis of thermionic space nuclear power reactor". International journal of energy research, 2019, vol 4.
8. Dai Z., Wang C., Zhang D., Tian W., Qiu S., Su G.H. "Design and analysis of a free-piston stirling engine for space nuclear power reactor". Nuclear Engineering and Technology (2020).
9. De Moura E.F., Ribeiro G.B., Henriques I. B. "Thermodynamic Analysis of a Stirling Cycle for Space Power Systems". 18th Brazilian Congress of Thermal Sciences and Engineering, Virtual conference, 2020.
10. De Moura E.F., Henriques I. B., Ribeiro G.B. "Thermodynamic Modeling and Exergy Analysis of a Stirling Cycle for Space Power Generation". ECOS 2020 - The 33rd International Conference on Efficiency, Cost, Optimization, Simulation and Environmental Impact of Energy Systems June 29-July 3, 2020, Osaka, Japan.
11. De Moura E.F., Henriques I.B., Ribeiro G.B. "Coupling of Finite Time Thermodynamic-Dynamic Models of a Stirling Engine for Nuclear Space Propulsion". 26 ABCM International Congress of Mechanical Engineering, November 22-26, 2021. Florianopolis, SC, Brazil.
12. De Moura E.F., Henriques I.B., Ribeiro G.B., "Finite-Time Thermodynamics and Exergy Analysis of a Stirling Engine for Space Power Generation, Thermal Science and Engineering Progress", (2021), doi: https://doi.org/10.1016/j.tsep.2021.101078.
13. De Moura E.F., Henriques I.B., Ribeiro G.B. "Thermodynamic-Dynamic coupling of a Stirling engine for space exploration" Thermal Science and Engineering Progress", (2022), doi: https://doi.org/10.1016/j.tsep.2022.101320.
14. El-Genk M.S. "Space nuclear reactor power system concepts with static and dynamic energy conversion". Energy Convers. Manage 49 (2008a) 402–411
15. El-Genk M.S. "Space reactor power systems with no single point failures". Nucl.Eng. Des. 238 (2008b) 2245–2255.
16. El-Genk M.S, Schriener. T.M. "Long operation life reactor for lunar surface power". Nucl. Eng. Des. 241 (2011) 2339–2352.
17. Fan S.;Li M.; Li S.; Zhou T.; Hu Y.; Wu S. "Thermodynamic analysis and optimization of a stirling cycle for lunar surface nuclear power system". Applied Thermal Engineering 111 (2017) 60-67.
18. Fan S. , Hu, Y., Li M. , Li S. , Zhou T. "Thermodynamic performance of lunar surface nuclear power system with heat sink temperature change in a rotational period". Applied Thermal Engineering 130 (2018) 127–134
19. Feng W., Lingen C., Fengrui S., Jiuyang Y. "Performance Optimization of Stirling Engine and Cooler Based on Finite-Time Thermodynamic". Chemical Industry Press, Beijing, 2008.
20. Gallo, B. M.; El-Genk, M. S. "Brayton rotating units for space reactor power systems". Energy Conversion and Management. v. 50, n. 9, p. 2210–2232, 2009.
21. Ribeiro G.B., Filho F.A.B., Guimarães L.N.F. "Thermodynamic analysis and optimization of a closed regenerative Brayton cycle for nuclear space power systems". Appl. Therm. Eng. 90 (2015) 250–257
22. Guimarães, L. N. F. "TERRA Project Update (2019), A Brazilian Nuclear Space Microreactor Development". International Nuclear Atlantic Conference –INAC 2019 XXIth Meeting on Nuclear Reactor Physics and Thermal Hydraulics –XXI ENFIR Santos, SP October 23rd, 2019

23. Haden, C. V., Collins, P. C., & Harlow, D. G. “Yield Strength Prediction of Titanium Alloys”. JOM, 67(6), 2015 1357–1361.
24. ISO 9809-1. “Gas cylinders - Refillable seamless steel gas cylinders - Design, construction and testing - Part 1: Quenched and tempered steel cylinders with tensile strength less than 1 100 MPa”.
25. Juhasz, A. “Heat Transfer Analysis of a Closed Brayton Cycle Space Radiator”. 5th International Energy Conversion Engineering Conference and Exhibit (IECEC), n. June, p. 25–27, 2007
26. Kwankaomeng S., Silpsakoolsook B., Savangvong P. “Investigation on Stability and Performance of a Free-Piston Stirling Engine”. 2013 International Conference on Alternative Energy in Developing Countries and Emerging Economies, 2013.
27. Lee S. M. , Jeffrey G. S. “Historical Review of Brayton and Stirling Power Conversion Technologies for Space Applications”. NASA/TM—2007-214976
28. Liao T., Lin J. “Optimum performance characteristics of a solar-driven Stirling heat engine system”. Energy Convers. Manage 97 (2015) 20–25.
29. Maxwell H.B. “Improving Free-Piston Stirling Engine Power Density”. NASA/TM—2016-219144.
30. Mcclure P.R, Poston D. Design and testing of small nuclear reactors for defense applications. Invited Talk to ANS Trinity Section (2013), Santa Fe, USA.
31. Reay D. A., Kew P. A., Mcglen R. J. Heat pipes. 6th. ed. Amsterdam: Elsevier, 2014
32. Romano, L. F. R., Ribeiro, G. B. Parametric evaluation of a heat pipe-radiator assembly for nuclear space power systems. Thermal Science and Engineering Progress, 2019, 100368.
33. Romano, L. F. R., Ribeiro, G. B. Cold-side temperature optimization of a recuperated closed brayton cycle for space power generation. Thermal Science and Engineering Progress, 2020, 100498.
34. Romano, L. F. R., Ribeiro, G. B. Optimization of a heat pipe-radiator assembly coupled to a recuperated closed Brayton cycle for compact space power plants. Applied Thermal Engineering, 2021, 117355.
35. Shubhash C. Kaushik ;Sudhir K.; Tyagi; Pramod Kumar. Finite Time Thermodynamics of Power and Refrigeration Cycles. Springer 1st ed, 2017.
36. Yaqi L., Yaling H., Weiwei H. “Optimization of solar-powered Stirling heat engine with finite-time thermodynamics”. Renew. Energy 36 (2011) 421–427.
37. Zohuri, B. “Heat Pipe Design and Technology”. (2016) doi:10.1007/978-3-319-29841 -2.

6. RESPONSIBILITY NOTICE

The Authors are the only responsible for the printed material included in this paper.